

---

# Embedded Haptic Control for Robotic Grasping using a Tactile Sensor System

---

**Thomas Kammerhofer**

Chair of Automation and Measurement  
Technical University of Leoben  
Peter-Tunner-Straße 25, 8700 Leoben  
thomas.kammerhofer@unileoben.ac.at

**Thomas Thurner**

Chair of Automation and Measurement  
Technical University of Leoben  
Peter-Tunner-Straße 25, 8700 Leoben  
thomas.thurner@unileoben.ac.at

## Abstract

Tactile sensing is essential for dexterous robotic manipulation, enabling reliable contact detection, grasp assessment, and safe interaction with delicate objects. In this work, we present a finger-shaped tactile sensor system based on a 2D array of MEMS barometric pressure sensors, designed to mimic the compliance and geometry of the human fingertip. The system integrates real-time contact force measurements utilizing the pressure sensor array, in combination with acceleration data from an onboard Inertial Measurement Unit (IMU), allowing both precise point-of-contact estimation and dynamic impact detection. A dedicated microcontroller ( $\mu\text{C}$ ) acts as a local processing and coordination node, responsible for closed-loop grasp and movement control, while a PC manages high-level communication between the  $\mu\text{C}$  and a robotic gripper. In addition, a hardware-level GPIO handshake between the control unit of a collaborative robot and the processing node enables deterministic synchronization between robotic arm positioning and grasp execution. Experimental validation of both the tactile sensor system and the robotic gripper control demonstrates robust operation across the conducted performance tests, with no malfunctions or object damage, as tactile feedback enables real-time grasping control throughout object manipulation. These results highlight the advantages of our tactile sensing solution as a cost-effective, versatile approach for enhancing robotic touch and advancing adaptive object-handling strategies.

## 1 Introduction

Dexterous object manipulation requires a continuous exchange of sensory information between the hand and the brain. In humans, this interaction is enabled by the highly specialized tactile sensing capabilities of the fingers, which allow not only the detection of contact forces but also the perception of object geometry, texture, and compliance. Through these rich sensory channels, humans adjust grip strength, adapt to unexpected disturbances, and execute delicate tasks such as tool use or object manipulation. Artificial replication remains a major challenge in robotics, where limited tactile feedback often constrains dexterity and adaptability. The integration of finger-shaped tactile sensors into robotics represents a significant advancement in robotic perception and manipulation capabilities, moving closer to the capabilities of the human sense of touch. These sensors provide essential tactile feedback, enhancing the robot's ability to interact effectively with its environment. Prior research shows that robots equipped with tactile sensors can achieve high levels of manipulation accuracy in uncertain environments (1; 2; 3), particularly when tactile data is exploited in closed-loop control for adaptive grasping and recognition of object properties (4; 5; 2; 6).

In addition to high sensitivity and resolution for accurate detection of contact forces, a mechanically soft and flexible sensor interface with a touch quality resembling human skin is highly advantageous, particularly for handling delicate items (such as e.g., fruits and vegetables) in agricultural harvesting,

processing, and supply logistics (7), (8). Moreover, as robotic systems increasingly evolve toward humanoid designs and human–robot interaction (9), mechanical properties such as softness and human-skin-like tactile perception are becoming critical for safe and natural interaction during object manipulation.

While tactile sensors have been an active field of research for more than a decade (10; 11), finger-based tactile sensors based on barometric pressure sensing are now emerging as a promising solution, driven by increased availability and affordability of low-cost MEMS barometric sensors. Early designs demonstrated that barometric sensors could be adapted to finger-like structures. Building on such work, later studies have explored utilizing MEMS-based barometric sensor arrays to enable high-resolution tactile mapping by detecting air pressure variations induced by external forces (12), while soft encapsulations mimicking the mechanical properties of human skin improved compliance and sensitivity (13; 14). This sensor information can be used not only for contact detection and force estimation, but also for slip detection (15) and dynamic contact interpretation (16), enabling direct control of an adaptive robotic gripper.

In this work, we present a finger-shaped tactile sensor system that combines a 2D array of MEMS-based barometric pressure sensors with a compliant fingertip design. The sensor array provides spatial pressure measurements across the fingertip, which are used to detect object contact and determine stable grasp conditions. The tactile signals are processed by an embedded controller and used for closed-loop robotic grasp control. This allows an integrated, in-line assessment of the current grasp and real-time adaptation of gripper behavior. To ensure reliable manipulation, a hardware-level handshake between the robot controller and the tactile processing unit is implemented to synchronize arm motion and grasp execution. Experimental evaluation demonstrates robust object interaction without damage, highlighting the potential of barometric tactile sensing as a cost-effective solution for tactile-driven robotic manipulation.

## 2 Tactile Sensor System for Robot Control

This section presents the architecture of the proposed tactile sensor system, starting with the sensing principle based on barometric pressure measurements and continuing with the supporting electronics for data acquisition and integration into the robotic control framework.

### 2.1 Tactile Sensor Concept

The developed tactile sensor solution, first introduced in (14), is designed to emulate selected mechanoreceptive functions of the human skin. The improved version, as presented in this paper is tailored to mimic the properties of the human finger. Each tactile sensor system, acting as an artificial finger, integrates 12 MEMS-barometric pressure sensors of type DPS368 (from Infineon Technologies AG (17)), hermetically sealed from the cell exterior by a flexible cell cover layer made from soft silicone (hardness Shore 25A). The shape (flat or finger-like) of this cell cover layer can be adapted depending on the target use case. A visual representation of the different types can be found in Figure 1, right, between the printed circuit boards (PCB) onto which the barometric pressure sensors are soldered, and the silicone cell cover layer to ensure a good sealing to the exterior and avoid cross-talk between individual sensor cells. The used tactile sensor system is conceptually illustrated in Figure 1, left, consisting of a 3D-printed mounting system (a), the printed circuit board (PCB) onto which the barometric pressure sensors are soldered (b), and the flexible cell cover (d). A resin-printed intermediate layer (c) was introduced between the PCB and the soft encapsulation to ensure proper sealing against the exterior and to avoid cross-talk between individual sensor cells. The sensors are arranged in a  $4 \times 3$  array with a sensor pitch of 10 mm to enable spatially resolved measurements of contact forces.

Each barometric pressure sensor in the tactile sensor system can be individually addressed via Inter-Integrated Circuit (I<sup>2</sup>C). Therefore, unique I<sup>2</sup>C addresses were pre-assigned and fused into the sensors during the assembly process. This setup allows multiple sensors to operate on the same communication bus without requiring additional multiplexing hardware. In addition, an ICM-42670-P six-degree-of-freedom (DoF) inertial measurement unit (IMU, from TDK InvenSense (18)) is integrated to capture motion-related data for vibration detection, and capture orientation changes and general robot-associated movements. With a sampling frequency of up to 1.6 kHz, the system can capture vibrations well beyond the perceptual frequency range of human skin ( $\approx 500$  Hz).

This capability makes it suitable to mimic the fast-adapting mechanoreceptors responsible for high-frequency vibration sensing in human touch.

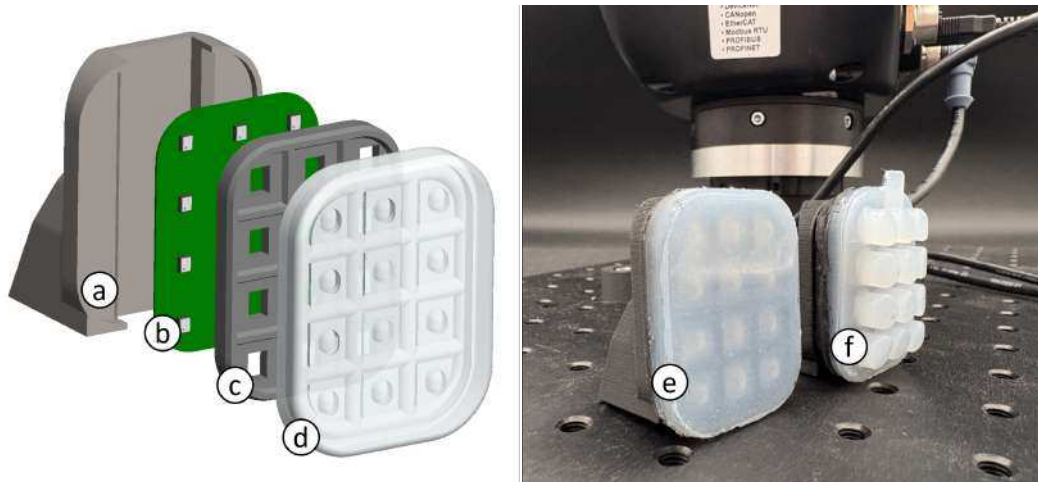


Figure 1: Conceptual illustration of the finger replacement for the robotic gripper, consisting of a 3D-printed mounting structure (a), the printed circuit board including sensors (b), a resin-printed intermediate layer (c), and a flexible cell cover layer (d). The developed prototypes can be seen in (e) and (f)

## 2.2 System Integration and Data Acquisition

A seamless integration of the tactile sensing system into the 3-Finger Adaptive Robot Gripper (from Robotiq (19)) can be achieved by replacing its original fingertips with custom 3D-printed ones (Figure 1). These replacements are designed to provide mounting surfaces and cable routing options for the tactile sensor modules, allowing the sensors to be directly attached without modifying the gripper's mechanical structure. The readout circuit for the tactile sensor array is placed close to the 3-Finger Adaptive Robot Gripper and is connected via a ribbon cable to the artificial finger. The readout circuit is centered around a CY8C6244-LQI microcontroller ( $\mu\text{C}$ , from Infineon Technologies AG (20)), which supports multiple communication protocols like I<sup>2</sup>C, Universal Asynchronous Receiver/Transmitter (UART) and Universal Serial Bus (USB), among others. The  $\mu\text{C}$  is responsible for high-speed data acquisition from the pressure sensor array at a sampling rate of 128 Hz, and from the IMU at a 1 kHz readout frequency, as well as for in-line data processing of the obtained data. It is important to note that this data rate is limited by the sensors rather than by the capabilities of the readout circuit.

By providing a virtual COM port, the system allows direct and efficient data exchange between the  $\mu\text{C}$  and a PC. For debugging measures, the sensor data can be transmitted to a PC for in-line assessment (in LabVIEW) or offline analyses (MATLAB) via UART.

The Robotiq 3-Finger Adaptive Gripper equipped with tactile sensor modules is mounted on a UR5 collaborative robot. While the gripper is controlled via USB communication by the  $\mu\text{C}$ , the overall manipulation task requires synchronization between arm positioning and grasp execution. To enable this coordination, a direct electrical interface is established between the UR5 controller and the tactile processing node using digital GPIO signals. The UR5 provides a position-confirmation signal once the predefined pick pose is reached, and the  $\mu\text{C}$  returns a confirmation signal after stable grasp detection.

## 2.3 Gripper Control

By utilizing the USB interface from the adaptive gripper, a communication path between the  $\mu\text{C}$  and the gripper can be established. However, as neither device can open its counterpart's communication port, an intermediate control layer is introduced. This layer is implemented on a PC and is responsible for managing the communication channels by opening the respective COM ports, forwarding messages between the  $\mu\text{C}$  and the gripper and properly closing the previously opened ports after

testing. A simple LabVIEW script fulfills this role, enabling reliable bidirectional communication and ensuring seamless integration of the tactile sensor system with the robotic gripper. For direct gripper control, a script consisting of at least two communication sections is necessary: an initialization section and a runtime phase in which the  $\mu\text{C}$  continuously sends positional commands to control the robot's movement. In this way, the Robotiq gripper can be activated and moved into desired positions, with possible variations in movement direction, movement speed and gripping force. These movements can therefore be adjusted based on the feedback obtained from the tactile sensor array. A more detailed description of the communication between  $\mu\text{C}$  and gripper can be found in section 3.

### 3 CONTROL FLOW

The control flow of the system is divided into two layers:  $\mu\text{C}$  firmware for sensor handling and real-time grasp control, and a LabVIEW script for communication and coordination with the robotic gripper.

#### 3.1 Microcontroller Firmware

The final control firmware directly runs on the CY8C6244-LQI  $\mu\text{C}$ . After board support package initialization, the system configures the USB interface for host PC communication and initializes the (I<sup>2</sup>C) bus for sensor access. Once all initializations are complete, it configures the DPS pressure sensors, including the output data rate, oversampling, continuous measurement mode, and offset correction.

Additionally, the IMU (ICM42670-P) and the robot gripper are initialized. For gripper control, the firmware issues an activation command to the gripper and continuously monitors its status until confirmation of successful activation is received. Once the handshake is complete, the system enters its main loop.

Within this loop, the  $\mu\text{C}$  continuously monitors both the state of the gripper and the robotic arm, as well as the tactile sensor array information and the accelerometer data. At the beginning of each grasping cycle, open-grip movement is executed, followed by a one second pause. Afterwards, the gripper closes until an object is detected, which can be determined by a measurable increase in the average cell pressure of the tactile sensor system. The pressure sensor array provides real-time pressure measurements with a resolution down to 1 Pa and sampling rates up to 128 Hz. This allows a precise estimation of contact points. Point-of-contact determination is further improved by correlating pressure changes with acceleration spikes captured by the IMU, indicating the moment of impact. Once contact is confirmed, the gripper reduces its closing speed until the tactile array signals that a predefined pressure threshold has been exceeded, indicating a stable grasp. Gripper motion then stops to prevent excessive force and thus potential damage to the manipulated object, and corrective actions such as reopening or repositioning can be triggered if needed. Subsequently, the GRIP\_STABLE indicator is transmitted, and the UR5 starts its movement.

These sensor values can be logged via UART or USB for thorough data analyses. For debugging purposes, the software is capable of transmitting full sensor datasets, including pressure values, acceleration readings, and processed features such as standard deviation through the virtual COM port or a separate UART to USB converter to the host PC.

#### 3.2 Robot- $\mu\text{C}$ Handshake

To ensure deterministic synchronization between the UR5 collaborative robot and the tactile processing node, a hardware-level handshake mechanism based on GPIO signals was implemented. To indicate that the robot has reached the predefined position, the UR5 controller asserts a logical HIGH signal ("ROBOT\_READY") on a dedicated GPIO line connected to the  $\mu\text{C}$ . Similarly, once the tactile sensor system detects a stable grasp condition, the  $\mu\text{C}$  asserts a logical HIGH signal ("GRIP\_STABLE") on a separate GPIO line connected to the UR5 control unit.

Upon detecting the ROBOT\_READY signal, the  $\mu\text{C}$  initiates the gripper closing procedure and continuously evaluates the tactile pressure data. Initial contact is detected when the average tactile sensor cell pressure exceeds the contact threshold, while a firm grasp is confirmed once the stability threshold is reached. At this point, the  $\mu\text{C}$  asserts GRIP\_STABLE to indicate successful object acquisition. The UR5 monitors this signal and resumes its programmed trajectory (e.g., lifting

motion) only after GRIP\_STABLE is detected. An overview about the described communication can be found in Figure 2, left.

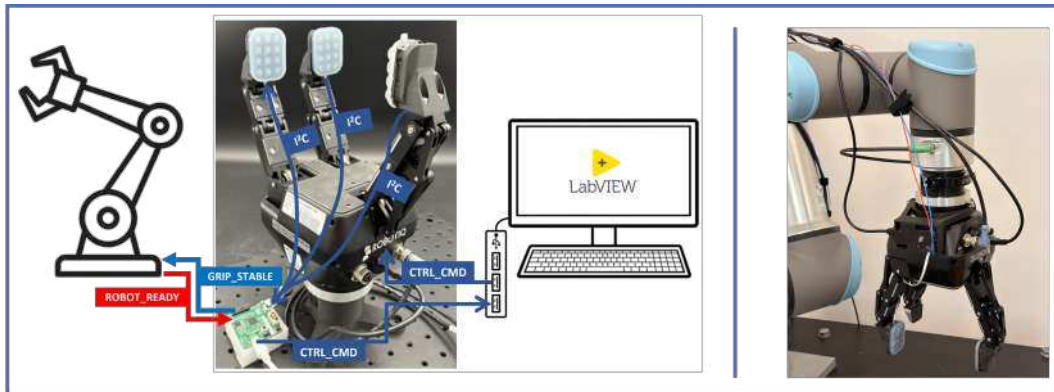


Figure 2: Left: Communication between individual components in the control loop. The  $\mu\text{C}$  is reading the sensor data, and sends corresponding control commands (CTRL\_CMD) via usb to the gripper. Movement coordination is handled via logical signals (GRIP\_STABLE / ROBOT\_READY) between the  $\mu\text{C}$  and the UR5. Right: Test setup using the tactile sensor systems attached to the Robotiq Adaptive 3-Finger Gripper and the UR5 collaborative robot.

### 3.3 Automation Script

A complementary LabVIEW script handles higher-level communication between the  $\mu\text{C}$  and the gripper. Its responsibilities are graphically depicted in Figure 3 and include:

- opening the COM ports,
- activating the gripper,
- flushing of  $\mu\text{C}$  queue after activation,
- forwarding movement commands to the gripper,
- forwarding positional feedback from the gripper to the  $\mu\text{C}$ , and
- closing the COM ports after test finalization.

While USB communication is used for command forwarding and status monitoring, motion–grasp synchronization is handled exclusively via GPIO signals to ensure deterministic timing. This separation of tasks ensures robust initialization, high-speed sensor readout, real-time decision-making for object detection, and a flexible communication pipeline that enables adaptive robotic manipulation based on tactile feedback.

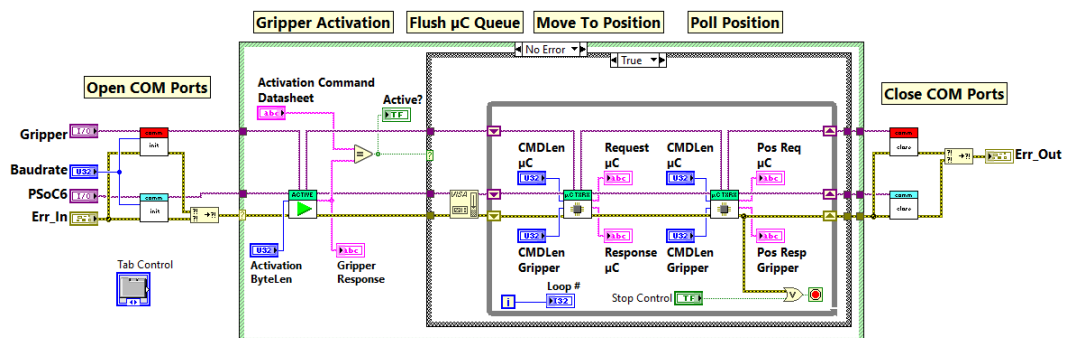


Figure 3: Overview of LabVIEW script used for PC-based automation of the gripper and  $\mu\text{C}$  interaction

## 4 Results

To evaluate the performance of the tactile sensing system, a series of manipulation cycles as described in section 3 was carried out by the Robotiq 3-Finger Gripper on various objects to evaluate the reliability of the algorithm. The objects varied in size, compressibility, weight, and surface texture. The gripping force was set to 20 N, resulting in a force of 6.6 N per finger, or 0.55 N per tactile sensor cell. It should be noted, however, that the force values are estimates and averages. An exact determination of force, or a relationship between applied force and measured cell pressure, can be established following a system characterization as described in (21).

Figure 4, left, shows the recorded average pressure change including the  $\pm 2\sigma$  range measured by the sensor array alongside the acceleration data from the IMU (Figure 4, right) from a test set resulting from grasping a fabric sample with a mass of approximately 150 g, corresponding to the typical mass of an average cotton T-shirt. During each manipulation, in which the grasping process lasted 6 s per iteration, distinct movement phases could be identified from the pressure and acceleration profiles. The closing phase (0.30–1.35 s) corresponds to the transport of the fingers toward the object. This is followed by a brief contact phase (1.35–1.60 s), marking the first interaction with the target and triggers a lower closing speed. The gripping phase (1.60–4.75 s) is initiated when an average change in pressure  $\Delta p = 0.25$  hPa was detected across all sensor cells, and the grip was defined as stable once the applied average pressure exceeded 3 hPa ( $\approx 0.55$  N). The releasing phase (4.75–4.85 s) reflected the loosening of grip, after which the opening phase (4.85–5.30 s) indicated the withdrawal and hand aperture increase. In total, 595 iterations were performed in this example, allowing for robust segmentation and statistical evaluation of the task phases.

The point of contact can be reliably determined from both the pressure signals and the acceleration

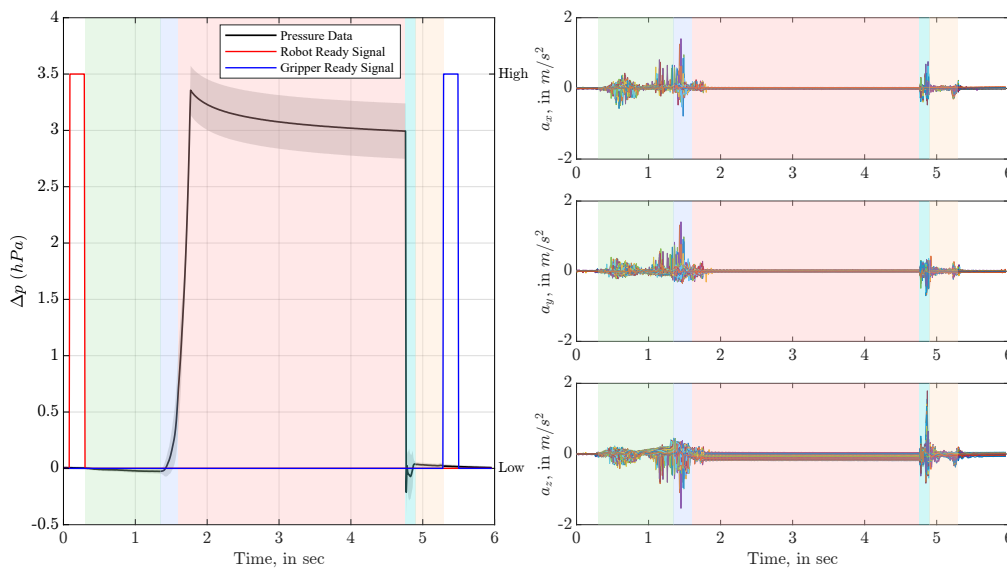


Figure 4: Pressure and acceleration patterns when grasping a compressible material. The grasping process can be subdivided into closing (green), contact (purple), grasping (red), releasing (cyan), and opening (orange) phases.

spike caused by the finger–object impact, and the accelerometer data can also be exploited in future object-handling strategies rather than relying exclusively on pressure information.

Across all conducted experiments, the system operated without malfunction and no objects were damaged due to excessive gripping force. The low-pressure threshold for contact detection, combined with the subsequent reduction in closing speed, consistently preserved the structural integrity of the grasped objects. No premature lifting motion was observed, and the UR5 resumed its trajectory exclusively after GRIP\_STABLE assertion, confirming reliable handshake operation.

## 5 CONCLUSION & FUTURE WORK

In this work, a tactile sensor system was developed and integrated into a Robotiq 3-Finger Gripper to enable sensor-driven robotic manipulation. Deterministic robot–grripper coordination via hardware handshakes was introduced to establish a reliable communication between the three essential system components:  $\mu\text{C}$ , gripper, and robotic arm. The system is centered around a  $\mu\text{C}$  that handles high-speed data acquisition from an array of pressure sensors and performs real-time data processing. Complementary information is obtained from an integrated IMU, allowing tactile events to be correlated with motion and vibration signals.

A seamless mechanical integration was achieved by replacing the gripper’s fingertips with custom 3D-printed parts, onto which the tactile sensor modules were mounted. This modular approach preserved the gripper’s functionality while enhancing it with high-resolution tactile feedback. The combination of USB-based communication and a LabVIEW control layer allowed reliable bidirectional data exchange between the  $\mu\text{C}$  and the gripper, enabling adaptive, sensor-based control strategies.

Experimental results demonstrated that the system can robustly detect object contact with high precision. Pressure changes as small as 1 Pa can be measured within individual sensor cells, and when combined with acceleration data, the point of contact can be estimated reliably. Plots of opening and closing iterations illustrated the strong correspondence between pressure transients and IMU signals, confirming the robustness of the approach.

Looking ahead, future work will focus on further increasing the temporal and spatial resolution of the tactile system. Pressure sensors capable of sampling at rates up to 500 Hz are already under consideration, which would further reduce the latency between different positional requests down to 2 ms.

In addition, the use of smaller sensor elements will reduce the sensor pitch, resulting in an increased spatial resolution of the tactile sensor system. In addition, the spatial resolution can be further increased by utilizing the interpolation algorithm, introduced in (22). Another important step will be the implementation of a slip detection algorithm, based on discontinuity detection (23; 24), directly on the  $\mu\text{C}$ . This will enable the gripper to autonomously detect and react to incipient slip conditions in real time, further enhancing its adaptability and robustness in manipulation tasks.

### Acknowledgments and Disclosure of Funding

The authors gratefully acknowledge the financial support provided by the Austrian Research Promotion Agency (FFG) and the Federal Ministry for Climate Action, Environment, Energy, Mobility, Innovation, and Technology under the project “MUTAVIA” (Project Nr. FO999922732).

### References

- [1] Z. Deng, Y. Jonetzko, L. Zhang, and J. Zhang, “Grasping force control of multi-fingered robotic hands through tactile sensing for object stabilization,” *Sensors*, vol. 20, p. 1050, 2020.
- [2] G. Sutanto, N. Ratliff, B. Sundaralingam, Y. Chebotar, Z. Su, A. Handa, and D. Fox, “Learning latent space dynamics for tactile servoing,” pp. 3622–3628, 2019.
- [3] D. Gomes, Z. Lin, and S. Luo, “Blocks world of touch: exploiting the advantages of all-around finger sensing in robot grasping,” *Frontiers in Robotics and Ai*, vol. 7, 2020.
- [4] R. Dahiya, P. Mittendorfer, M. Valle, G. Cheng, and V. Lumelsky, “Directions toward effective utilization of tactile skin: a review,” *Ieee Sensors Journal*, vol. 13, pp. 4121–4138, 2013.
- [5] S. Tian, F. Ebert, D. Jayaraman, M. Mudigonda, C. Finn, R. Calandra, and S. Levine, “Manipulation by feel: touch-based control with deep predictive models,” pp. 818–824, 2019.
- [6] H. Yousef, M. Boukallel, and K. Althoefer, “Tactile sensing for dexterous in-hand manipulation in robotics—a review,” *Sensors and Actuators a Physical*, vol. 167, pp. 171–187, 2011.
- [7] Y. A. AboZaid, M. T. Aboelrayat, I. S. Fahim, and A. G. Radwan, “Soft robotic grippers: A review on technologies, materials, and applications,” *Sensors and Actuators A: Physical*, vol. 372, p. 115380, 2024. [Online]. Available: <https://www.sciencedirect.com/science/article/pii/S0924424724003741>

- [8] P. Beckerle, R. Kõiva, E. A. Kirchner, R. Bekrater-Bodmann, S. Dosen, O. Christ, D. A. Abbink, C. Castellini, and B. Lenggenhager, “Feel-Good Robotics: Requirements on Touch for Embodiment in Assistive Robotics,” *Frontiers in Neurorobotics*, vol. 12, p. 84, Dec. 2018.
- [9] Y. Tong, H. Liu, and Z. Zhang, “Advancements in Humanoid Robots: A Comprehensive Review and Future Prospects,” *IEEE/CAA Journal of Automatica Sinica*, vol. 11, no. 2, pp. 301–328, Feb. 2024. [Online]. Available: <https://ieeexplore.ieee.org/document/10415857/>
- [10] R. S. Dahiya, G. Metta, M. Valle, and G. Sandini, “Tactile sensing—from humans to humanoids,” *IEEE Transactions on Robotics*, vol. 26, no. 1, pp. 1–20, 2010.
- [11] J. A. Fishel and G. E. Loeb, “Sensing tactile microvibrations with the biotac — comparison with human sensitivity,” in *2012 4th IEEE RAS EMBS International Conference on Biomedical Robotics and Biomechatronics (BioRob)*, 2012, pp. 1122–1127.
- [12] Y. Tenzer, L. P. Jentoft, and R. D. Howe, “The feel of mems barometers: Inexpensive and easily customized tactile array sensors,” *IEEE Robotics Automation Magazine*, vol. 21, no. 3, pp. 89–95, 2014.
- [13] T. Clercq, A. Sianov, and G. Crevecoeur, “A soft barometric tactile sensor to simultaneously localize contact and estimate normal force with validation to detect slip in a robotic gripper,” *IEEE Robotics and Automation Letters*, vol. 7, pp. 11 767–11 774, 2022.
- [14] T. Thurner, T. Kammerhofer, B. Reiterer, and M. Hofbauer, “Tactile sensor solution with MEMS pressure sensors in industrial robotics,” *e & i Elektrotechnik und Informationstechnik*, vol. 140, no. 6, pp. 541–550, Oct. 2023.
- [15] T. Kammerhofer, D. Ninevski, M. Danner, and T. Thurner, “Real-time slip detection for robotic tactile sensors via discontinuity detection,” in *2026 IEEE International Instrumentation and Measurement Technology Conference (I2MTC)*, 2026, **to appear**.
- [16] A. Grover, P. Nadeau, C. Grebe, and J. Kelly, “Learning to detect slip with barometric tactile sensors and a temporal convolutional neural network,” in *2022 International Conference on Robotics and Automation (ICRA)*, 2022, pp. 570–576.
- [17] *DPS368 - Digital XENSIV™ Barometric Pressure Sensor*, Infineon Technologies AG, 2019, rev. 1.1.
- [18] *ICM-42670-P - High Performance 6-Axis MotionTracking™ IMU*, InvenSense, a TDK Group Company, 2021, rev. 1.0.
- [19] *Robotiq 3-Finger Adaptive Robot Gripper Instruction Manual*, Robotiq, 2018, rev. 271118.
- [20] *PSoC™ 62 MCU*, Infineon Technologies AG, 2024, rev. \*M.
- [21] T. Kammerhofer, J. Handler, and T. Thurner, “Performance evaluation and characterization of an industrial tactile sensor solution,” in *IECON 2025 – 51st Annual Conference of the IEEE Industrial Electronics Society*, 2025, pp. 1–7.
- [22] T. Kammerhofer, D. Ninevski, and T. Thurner, “Advanced tactile sensor solution with spline surface interpolation for robotics,” in *2025 IEEE International Instrumentation and Measurement Technology Conference (I2MTC)*, 2025.
- [23] D. Ninevski and P. O’Leary, “Detection of derivative discontinuities in observational data,” in *Advances in Intelligent Data Analysis XVIII*, M. R. Berthold, A. Feelders, and G. Kreml, Eds. Cham: Springer International Publishing, 2020, pp. 366–378.
- [24] D. Ninevski and P. O’Leary, “A convolutional method for the detection of derivative discontinuities,” in *2020 21th International Carpathian Control Conference (ICCC)*, 2020, pp. 1–5.